



AGNs in the XMDS: spectral energy distributions and X-ray colors

M. Tajer^{1,2}, G. Trinchieri¹, L. Chiappetti³, L. Maraschi¹ and D. Maccagni³
on behalf of the XMDS and VVDS collaborations

¹ INAF – Osservatorio Astronomico di Brera, via Brera 28, 20121 Milano, Italy

² Università degli Studi di Milano – Bicocca, Dipartimento di Fisica, P.za della Scienza 3, 20126 Milano, Italy

³ INAF - IASF Sezione di Milano “G. Occhialini” - via Bassini 15, 20133, Milano, Italy
e-mail: tajer@brera.mi.astro.it

Abstract. We present the results of the analysis of spectral energy distributions (SEDs) and optical and X-ray colors of 189 X-ray sources detected at $> 4\sigma$ in the XMM Medium Deep Survey (XMDS), identified with an optical counterpart in the VIMOS VLT Deep Survey, having a good multiwavelength photometry. We find that the optical SEDs show a skewed distribution of $B - I$ color, with a peak in the range 0.3 - 1.2 which includes about 65% of the objects, and a flat tail in the range 1.3 - 3 populated by the remaining 35% of objects. Notably the two groups have different distributions also in the X-ray color-color plane. The data suggest that simply absorbed sources occur within the $B - I > 1.3$ group while some of the $B - I < 1.3$ sources exhibit composite X-ray spectra with both a hard and a soft component.

Key words. X-ray: surveys – X-ray: AGNs

1. Introduction

The XMM Medium Deep Survey (XMDS, see Chiappetti et al. 2005) consists of 19 *XMM - Newton* contiguous pointings of 20 ks typical exposure and aims at obtaining a deep multi-wavelength coverage of a contiguous area of about 3 deg².

The study of Spectral Energy Distributions (SEDs), using data at several wavelengths, can give useful information about the nature of sources, allowing e.g. a broad distinction between type 1 (broad emission lines) and type 2 (narrow emission lines) AGNs or normal

galaxies, even without optical spectroscopic information (see e.g. Franceschini et al. 2005).

In the present work we present results from X-ray and optical photometric data; analysis of infrared data is in progress.

We detected 536 X-ray sources with a significance $> 4\sigma$ in at least one of the energy bands 0.3–0.5, 0.5–2, 2–4.5, 4.5–10 and 2–10 keV. Detailed information on observations and data reduction is reported in Chiappetti et al. (2005).

About 1 deg² of the XMDS area is covered by the VIMOS VLT Deep Survey (VVDS), both UBVRI photometry (Le Fèvre et al. 2004) and multi - object spectroscopy (Le Fèvre et al.

Send offprint requests to: M. Tajer

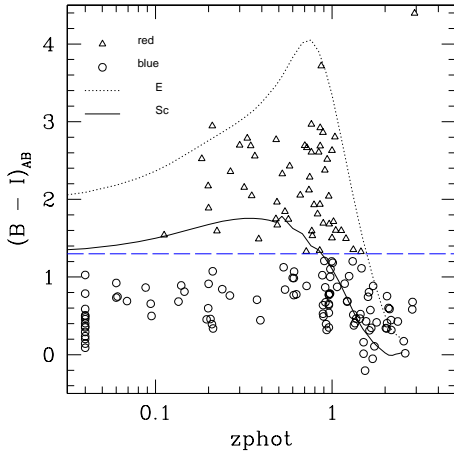


Fig. 1. $B-I$ distribution of sources in the 4σ VVDS sample as a function of photometric redshift. Circles are “blue” objects, triangles are “red” objects (see text). The solid and dotted lines are the evolutionary tracks for an Sc galaxy and an elliptical galaxy, respectively, from Poggianti (1997). The dashed line marks the division between red and blue objects.

2005). A search of optical counterparts of the 286 X-ray sources in the VVDS area yielded 232 reliable identifications at $R_{AB} \leq 24$ (the 4σ VVDS sample, see Chiappetti et al. 2005). Of these, 189 have reliable optical photometry.

2. Optical colors

We used X-ray and optical photometric information to construct SEDs for all the 189 sources. We found essentially two types of objects, based on the shape of the SED in the optical region: about 2/3 of sources show a “flat” optical SED, with comparable fluxes in the UBVRI bands, while the remaining show a “steep” SED, with optical flux decreasing from the I to the U band. The distribution of the observed $B-I$ color of our sample shows a large peak for $B-I \leq 1.3$, corresponding to sources with a flat SED, and a tail extending up to $B-I \geq 3$, for sources with a steep SED. We therefore took $B-I = 1.3$ as a dividing line and will briefly call “blue” the objects with $B-I < 1.3$, and “red” those with $B-I > 1.3$.

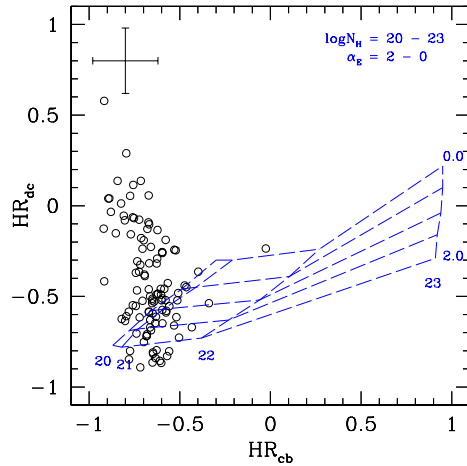


Fig. 2. X-ray color - color plot for blue objects. Energy bands involved are: 0.5 – 2 (B), 2 – 4.5 (C) and 4.5 – 10 keV (D). Superimposed to points is the grid of loci for power law spectra with index α_E and column density N_H (at $z = 0$). Typical error bars are also shown.

In Fig. 1 we show the $B-I$ color vs the VVDS photometric redshift for our sources, along with the evolutionary tracks for an Sc and an elliptical galaxy, from Poggianti (1997). For $z_{phot} \leq 1$ both galaxy tracks lie above $B-I = 1.3$, while for $z > 1$ the distinction is blurred. It is therefore reasonable to suppose that for red sources the optical emission could be due to galactic starlight, while for blue objects the optical contribution from the AGN dominates. Our rough classification finds support in results published by Franceschini et al. (2005), who present SEDs of *Chandra* sources seen in the *Spitzer* Wide-area Infrared Extragalactic (SWIRE) survey. They fit a number of spectral templates to SEDs to determine spectral categories (type 1 AGN, type 2 AGN, normal galaxy...) and it appears that type 1 AGNs have flatter SED and bluer optical colors than type 2 AGNs and galaxies, which show similar SEDs.

Since $> 80\%$ of our sources have an X-ray to optical ratio typical of canonical AGNs (see Chiappetti et al. 2005, and references therein), we expect that for nearly all sources the X-ray emission originates from the AGN and that red

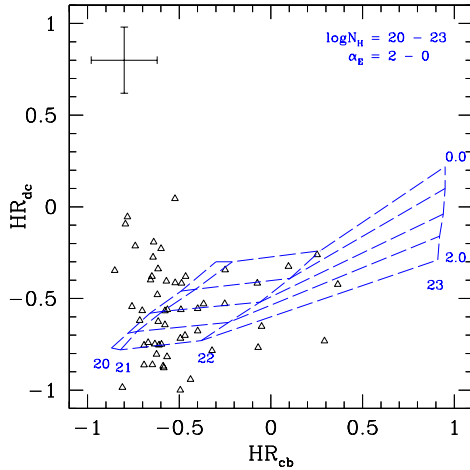


Fig. 3. Same as Fig. 2 for red objects.

objects contain a significant fraction of type 2 AGNs. This hypothesis is supported by the fact that, while for the blue population we do not find a correlation between X-ray to optical ratio and X-ray luminosity, for red objects the X-ray to optical ratio increases with L_X , as observed by Fiore et al. (2003) for type 2 AGNs.

The available optical spectroscopy (for ~ 20 objects) confirms that red objects show typical galaxy spectra, often with narrow emission lines, while broad emission lines are present only in blue objects.

3. X-ray colors

We found a relation between optical and X-ray colors. In Fig. 2 and 3 the hardness ratios in different bands of blue and red objects respectively are compared with the expectations of simple absorbed power law models ($\alpha = 0 - 2$,

$N_H = 10^{20} - 10^{23} \text{ cm}^{-2}$). The two distributions appear significantly different: 9 of the 65 red sources (14%) have $HR_{cb} > -0.3$, suggesting X-ray absorption ($N_H \geq 10^{22} \text{ cm}^{-2}$), while only one of the 124 blue objects ($\sim 1\%$) lie in this portion of the plot.

On the other hand, sources with $HR_{cb} < -0.5$ and $HR_{dc} > -0.2$, mostly blue, cannot be explained by the simple power law spectral model, even taking into account large errors: we suggest that they have a concave spectral shape, resulting from a hard or absorbed power law plus a soft component.

We performed X-ray spectral analysis where possible and confirmed these findings: sources showing high values of HR_{cb} have $N_H \geq 10^{22} \text{ cm}^{-2}$ (indeed a lower limit to N_H because a redshift $z = 0$ was assumed in the X-ray spectral analysis) and are a significant fraction of red objects ($\sim 20\%$), while spectra of sources with $HR_{cb} < -0.5$ and $HR_{dc} > -0.2$ show a significant excess of counts for $E > 5 \text{ keV}$ with respect to the simple absorbed power law model. Unfortunately the number of net counts in these sources is too small to perform a significant fit, but a two power law model, with the first component having N_H fixed to the galactic value and a second highly absorbed component ($N_H \geq 10^{24} \text{ cm}^{-2}$) gives reasonable results.

References

- Chiappetti, L. et al. 2005, A&A accepted, astro-ph/0505117
- Fiore, F. et al. 2003, A&A 409, 79
- Franceschini, A. et al. 2005, AJ 129, 2074
- Le Fèvre, O. et al. 2004a, A&A, 417, 839
- Le Fèvre, O. et al. 2005, A&A accepted, astro-ph/0409133
- Poggianti, B. M., 1997, A&AS, 122, 399